Agricultural and Forest Meteorology 368 (2025) 110525

Contents lists available at ScienceDirect

Agricultural and Forest Meteorology

journal homepage: www.elsevier.com/locate/agrformet

Fog presence and ecosystem responses in a managed coast redwood forest

Julia Petreshen [a], Salli F. Dymond [b,*], Elizabeth T. Keppeler [c], Scott T. Allen [d], Joseph W. Wagenbrenner [e]

[a] Department of Earth and Environmental Sciences, University of Minnesota Duluth, 1114 Kirby Dr., Duluth, MN, USA
[b] School of Forestry, Northern Arizona University, 200 E Pine Knoll Dr., Flagstaff, AZ, USA
[c] USDA Forest Service Pacific Southwest Research Station, 802 N. Main St., Fort Bragg, CA, USA
[d] University of Nevada Reno, Department of Natural Resources and Environmental Science, 1164 N. Virginia St., Reno, NV, USA
[e] USDA Forest Service, Pacific Southwest Research Station, 1700 Bayview St., Arcata, CA, USA

ARTICLE INFO

Keywords:
Fog
Sequoia sempervirens
Transpiration
Soil moisture
Streamflow
Sap flow
Harvest

ABSTRACT

Fog inundation along California's Coast Range creates microclimates that support coast redwood (*Sequoia sempervirens* (D. Don) Endl.) forests during the summer drought period. With changes in land use and climate, the coast redwood ecosystem is more susceptible to increased drought stress. Thus, understanding the role of fog in relieving drought stress is important to manage the remaining coast redwood forests. Fog presence, other climatic conditions, soil moisture, and sap flow were monitored at the Caspar Creek Experimental Watersheds in northwestern California over the 2020, 2021, and 2022 fog seasons (1 May – 30 Sep). Observations were recorded at shoulder and ridge topographic positions in harvested and unharvested third-growth forest to examine 1) temporal and spatial distribution of fog, 2) soil moisture responses to fog drip, and 3) the influence of fog on transpiration and streamflow. Fog presence was found to vary across the landscape with no significant relationship to harvesting. Leaf wetness as a result of fog was higher at the shoulder position than at the ridge of the hillslope. At all study sites, fog events tended to result in small increases in soil moisture or reduced withdrawals of soil moisture, albeit variably throughout the fog season. All sites displayed lower transpiration rates during fog periods and streamflow recession rates were similarly reduced. Overall, this research suggests that the occurrence of fog is ecologically and hydrologically important at the Caspar Creek Experimental Watersheds, and those effects are influenced by topography but not apparently by forest density.

1. Introduction

Fog inundation creates microclimates that result in unique ecological communities. One of the most considerable influences of fog on ecosystem microclimates is alleviating plant water stress; this sometimes generates distinct ecological communities across small geographic areas (e.g., Dawson, 1998; Ewing et al., 2009). Along the eastern Pacific Ocean, the upwelling of the California Current causes temperature inversions and drives fog formation along the coast of California. Onshore winds and temperature differences between the ocean and land drive fog inland, which relieves seasonal summertime droughts that are characteristic of the region's Mediterranean climate. Typically, vegetation in Mediterranean climates is adapted to seasonal summertime droughts, as winter rains are often the primary input to the annual water budget (Arkley, 1981; Klos et al., 2018). However, the frequent fog and stratus clouds that form along the California coast during the dry summer months variably interact with landscape and vegetation to create unique microclimates that support coast redwood forests. Dominated by the tallest living tree species on Earth, *Sequoia sempervirens* ((D. Don) Endl.), the narrow distribution of the coast redwood forest is limited to the fog-prone zone along the California coast, locally referred to as the "fog belt" where habitat suitability for coast redwood is strongly linked to fog frequency (Francis et al., 2020). *S. sempervirens* growth efficiency and drought sensitivity is correlated to summer fog frequency along a north-to-south latitudinal gradient, with higher growth efficiency and reduced drought sensitivity at more fog-prone sites (Sillett et al., 2022).

Fog presence can relieve tree water stress through various mechanisms, such as reducing the amount of water lost through evapotranspiration, supplying water to plants through foliar uptake, supplementing soil moisture through fog drip, and reducing vapor pressure deficit via

* Corresponding author.
E-mail addresses: petreshenj@gmail.com (J. Petreshen), salli.dymond@nau.edu (S.F. Dymond), elizabeth.keppeler@usda.gov (E.T. Keppeler), scottallen@unr.edu (S.T. Allen), joseph.wagenbrenner@usda.gov (J.W. Wagenbrenner).

https://doi.org/10.1016/j.agrformet.2025.110525
Received 1 November 2024; Received in revised form 20 March 2025; Accepted 24 March 2025
Available online 8 April 2025
0168-1923/

cooler temperatures and increased humidity. Reduction in plant transpiration during fog events has been demonstrated via sap flow measurements — sap flow in *S. sempervirens* is often reduced and, in some cases, reversed during fog events (Burgess and Dawson, 2004; Simonin et al., 2009). Sap flow reversal indicates fog water is being directly absorbed through foliage, which has been observed in 80 % of the dominant overstory and understory species in coast redwood forests (Limm et al., 2009). This absorbed fog water may then be used to refill desiccated plant tissues and maintain or enhance growth during periods of low rainfall, further demonstrating the importance of fog to the coast redwood forest. These impacts on tree water use also suggest the importance of fog to the overall water balance and provisioning of stream water.

Accumulated fog water on foliage can also coalesce to large droplets and generate fog drip. Fog drip contributes to water stored in the soil, where it is further available for plants via root uptake. Fog drip has been a long-studied phenomenon along the California coast due to its role in relieving seasonal drought (Means, 1927; Oberlander, 1956; Azevedo and Morgan, 1974; Dawson, 1998), increasing soil moisture (Ewing et al., 2009; Carbone et al., 2011), and increasing or summertime streamflow recession (Sawaske and Freyberg, 2015). When fog drip is observed, it often improves plant water status by increasing soil moisture (Dawson, 1998; Ewing et al., 2009; Fischer et al., 2016). However, the magnitude and extent of fog drip varies across studies and is influenced by a range of site characteristics (Ingraham and Matthews, 1995; Dawson, 1998; Ewing et al., 2009; Carbone et al., 2013; Fischer et al., 2016; Cárdenas et al., 2017). Fog drip is generally found to increase with elevation and decrease with distance from the coast (Holder, 2003; Fischer and Still, 2007; Fischer et al., 2009). Since wind is the primary driver of advective fog, higher wind speeds coming from the northwest are often linked to higher rates of fog drip (Johnstone and Dawson, 2010; Pryet et al., 2012; Hiatt et al., 2012). This interplay of meteorology and topography influences fog dynamics in forests and thus fog drip quantity and timing.

Fog interception and its volumetric input to the ecosystem water balance depends on many factors, including local topography, climate, and forest structure. Changes in land use by natural or anthropogenic forces may alter forest structure and change patterns of fog formation and deposition in an ecosystem. Timber harvest within the coast redwood forest is a common land use practice which reduces stand density and can potentially impact fog dynamics. The relationship between stand density and fog interception has been well studied along the Pacific coast (Harr, 1982; Ingwersen, 1985; Dawson, 1998; Keppeler, 2007) and around the world (Ataroff and Rada, 2000; Barbosa et al., 2010). However, the connection between forest structure and fog remains unclear. Some studies indicate that the greatest fog interception and drip occur at forest edges based on the direct exposure to fog-laden winds (Ewing et al., 2009; Keppeler, 2007). Other studies show that fog drip is greatest in closed canopy systems, where canopy surfaces increase interception and reduce the evaporation of fog drip (Dawson, 1998; Barbosa et al., 2010). Regardless, warming sea-surface temperatures along the California coast may be driving a decline in summertime fog (Johnstone and Dawson, 2010; Werner et al., 2022), which has profound implications for the health and distribution of the coast redwood forests and watersheds.

Given the role of fog in maintaining the vitality of the redwood forest and that many of these forests are actively managed for density and structure, there is a pressing need to understand how fog drip and its role in relieving the effects of seasonal drought interact with forests of varying structures. This study expands upon our current understanding of spatiotemporal fog-forest interactions and examines the influence of timber harvest on fog drip in a managed third-growth coast redwood forest. The relationship between fog, forest structure, and topography are explored by examining 1) leaf wetting caused by fog presence, 2) soil moisture following fog events, 3) transpiration rates in *S. sempervirens* during fog presence, and 4) streamflow response to fog-related effects.

2. Methods

2.1. Caspar Creek Experimental Watersheds

The Caspar Creek Experimental Watersheds (CCEW; 39°21′N, 123°44′W) are located in northwestern California, USA on the Jackson Demonstration State Forest (Richardson et al., 2021). Historically, old-growth forests in the region were heavily logged from the 1860′s until around 1904. After the CCEW were established, approximately $^2/_3$ of the second-growth forest in the Caspar Creek South Fork watershed was removed via selection harvest between 1971 – 1973 as part of the first experimental treatment. Another experimental harvest occurred in 2017 – 2019 and reduced stand densities in South Fork sub-watersheds by 0 to 76 percent (Dymond et al., 2021*a*).

The climate at CCEW is classified as Mediterranean (Köppen csbn), with wet, mild winters and relatively dry, cool summers. Low-intensity rainfall delivers 90 % of annual precipitation between the months of October and April, with a mean annual depth of 1168 mm between the years of 1989 – 2018 (Dymond et al., 2021*a*). Summers receive little precipitation—averaging 120 mm over the five-month May--through-September period—but experience frequent fog events which typically develop at night, extend up to 16 km inland, and dissipate by midday. Located 7 km from the Pacific Ocean, seasonal fluctuations in air temperatures at CCEW are minimal due to the coastal influence. Mean monthly air temperatures fall between 6.7 – 15.6 °C. Elevations in the watersheds range between 37 and 320 m. Soils at CCEW developed from the weathering of marine sandstone to produce well-draining clay loams in the Ultisol and Alfisol soil orders (Henry, 1998). The dominant tree species at CCEW are coast redwood (*Sequoia sempervirens* (D. Don) Endl.) and Douglas-fir (*Pseudotsuga menziesii* (Mirb.) Franco). Also present in lower quantities are grand fir (*Abies grandis* (Dougl. ex D.Don) Lindl.), western hemlock (*Tsuga heterophylla* (Raf.) Sarg.), tanoak (*Lithocarpus densiflorus* (Fook. and Arn.) Rohn), and red alder (*Alnus rubus* Bong.) (Cafferata and Reid, 2013). Understory vegetation includes evergreen huckleberry (*Vaccinum ovatum* Pursh), Pacific rhododendron (*Rhododendron macrophyllum* D. Don), and sword fern (*Polystichum munitum* (Kaulf.) Presl.) (Henry, 1998; Kassuelke et al., 2022).

2.2. Study sites and instrumentation

This study uses four 1/20th ha study sites that are part of a larger study on the impacts of timber harvest on forest watershed processes (Dymond et al., 2021*a*). The Williams (WIL) sub-watershed received no harvest in the most recent experiment and is referred to as the “forested” sub-watershed in this study. In the 24 ha “harvested” Ziemer (ZIE) sub-watershed, 76 % of the pre-treatment basal area was removed from the 1/20th ha study plots as well as catchment-wide in 2017 (Fig. 1). For this study, one site was instrumented at the shoulder and ridge of the hillslope in each sub-watershed to study fog interception, yielding four study sites. Site characteristics and distribution of overstory species at study sites were measured in 2019 (Table 1). A nearby meteorological station (MET) recorded 10-minute precipitation in a clearing using an Ott-Pluvio weighing rain gage (0.025 mm resolution) over the duration of the study (Fig. 1).

Instruments to measure fog conditions were installed at the four study sites in March and June 2020. To monitor the occurrence and infiltration of fog drip from the canopy, SoilVUE10 soil moisture sensors (Campbell Scientific, Logan, UT, USA) were installed at three locations around one *S. sempervirens* tree at the center of each plot: within 1 m of the bole (“bole”), near the canopy drip edge (“drip edge”), and in a nearby opening (“open”). Openings at the forested locations were difficult to find, so the best suitable position for the “open” sensor was one with a gap in canopy cover. Sensors recorded volumetric water content (VWC) of soils at 5 cm and 10 cm depths. LAI was measured at each plot and in canopy openings using LAI-2200C Plant Canopy Analyzer (LI-COR Environmental, Lincoln, NE, USA); LAI values are

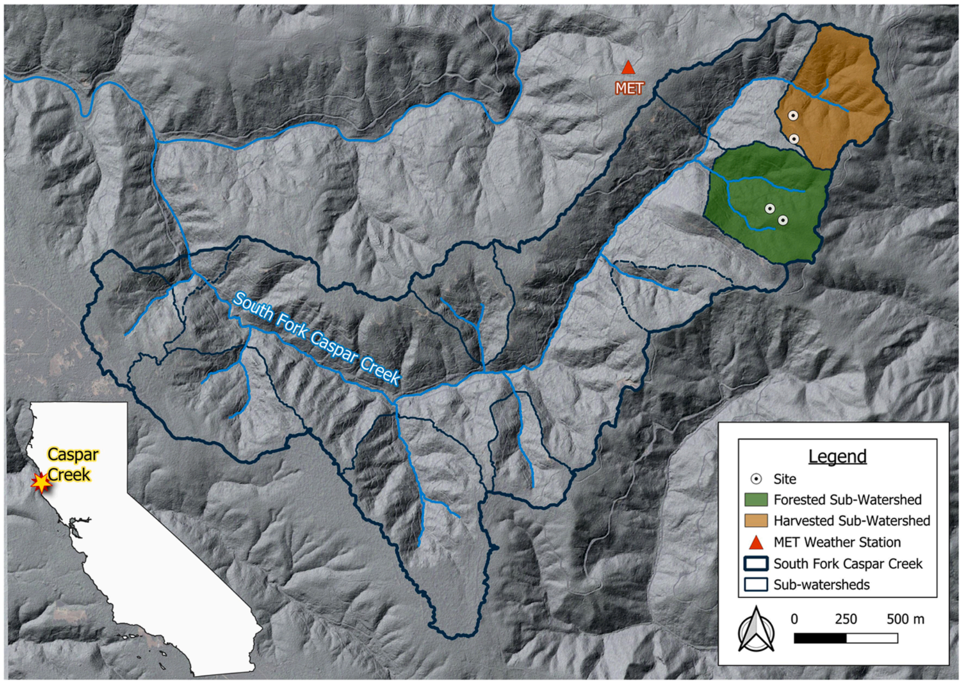

Fig. 1. The South Fork Caspar Creek is located on the north coast of California. This study consists of four sites, located at ridge and shoulder hillslope positions within one forested and one harvested sub-watershed. The instrumented sites are part of a larger hillslope transect study (see Dymond et al., 2021a).

Table 1
Physical characteristics and overstory species distributions of study sites (from Dymond et al. 2021a). Species acronyms refer to coast redwood (RW), tanoak (TO), Douglas-fir (DF), grand fir (GF), and rhododendron (RD). LWS refers to the leaf wetness sensor that was deployed at each site.

Treatment	Attribute	Forested (WIL)		Harvested (ZIE)	
Position		*Shoulder*	*Ridge*	*Shoulder*	*Ridge*
Physical Characteristics	Elevation (m)	252	274	248	270
	Aspect (°)	357	288	351	294
	Slope (%)	55	25	28	19
	Basal Area (m^2 ha^{-1})	32	20	2	6
	LAI	6.7 ± 0.1	7.9 ± 0.1	0.6 ± 0.1	1.2 ± 0.1
Species Distribution (% of Total Basal Area)	RW	27.9	87.4	84.2	83.5
	TO	0.3	1.2	15.8	16.4
	DF	69.9	4.1	0	0
	GF	0.8	4.3	0	0
	RD	1	3	0	0
LWS Tree Characteristics	Species	DF	RW	DF	RW
	Height (m)	42.4	25.9	41.5	26.8
	Live Crown Ratio	0.29	0.59	0.46	0.49
Sap Flux Tree Characteristics (measured in 2020)	Species	RW	RW	RW	RW
	DBH (cm)	41.9	38.9	38.9	31.8
	Height (m)	20.8	22.0	24.7	17.8
	Live Crown Ratio	40.2	53.4	62.6	50.1

based on a 106° view angle which better approximates LAI than using the full view (Weiss et al., 2004). The harvested ridge site bordered the forested sub-watershed to the west, so an easterly azimuth (60 – 110°) was used for installing the soil moisture sensors relative to the study tree to avoid possible edge effects. The remaining sites were installed at the same azimuth and contour of the tree at the center of the site.

Leaf wetness was used as an indicator of fog presence. One tree at each study site was instrumented with a Campbell Scientific leaf wetness sensor (LWS; Campbell Scientific, Logan, UT, USA) located approximately 6.1 m (20 ft) above the ground and attached to the bole by a 0.3 m bracket (Fig. 2). This sensor was oriented in a northwesterly direction (azimuth of ~ 315°) to face the prevailing summer winds in this region (Williams et al., 2008; Rastogi et al., 2016). Due to limited cable lengths, the LWS sensor was installed on different tree species at each site (Table 1). At each site, meteorological conditions were recorded in the canopy of the selected tree at 9 to 25 m above the ground. Wind conditions were measured by an anemometer (03002 R.M. Young Wind Sentry Set, Campbell Scientific Inc., Logan, UT, USA) attached to the trunk within the crown. A temperature and relative humidity sensor (EE181, Campbell Scientific Inc., Logan, UT, USA) housed in a radiation shield (RAD10E, Campbell Scientific Inc., Logan, UT, USA) was paired with each anemometer. All sensors were secured to a mounting frame at an azimuth of ~ 315° to face prevailing summer winds. Leaf wetness, wind speed and direction, temperature, relative humidity, and soil

Fig. 2. Photograph of leaf wetness sensor (LWS) secured to a bracket and mounted at a height of 6.1 m in a S. sempervirens tree at the harvested ridge site.

moisture were recorded at 15 min intervals via a CR1000 datalogger (Campbell Scientific Inc., Logan, UT, USA).

In 2016, one SFM1 Sap Flow Meter (ICT International Pty Ltd, Armidale, Australia) was installed at a height of 1.37 m on one *S. sempervirens* study tree at the center of each site (Dymond et al., 2021a). The SFM1 meter measures sap flow velocity using the heat-ratio method (HRM) — this method was chosen due to its ability to detect both zero-flow and reverse sap flow. Study trees selected were of a similar diameter class, (31.7 cm to 41.9 cm at the time of installation), were in a dominant or co-dominant canopy position, and were free from bole or canopy diseases or damage. Sap flow velocity (cm hr^{-1}) was measured at 10-minute intervals. A sensor measuring photosynthetically active radiation (PAR; Licor Quantum LI190SB, Lincoln, NE) on a 10-minute interval, was installed 2.5 m south of the sap flux tree.

We used 10-minute rainfall data collected from a weighing precipitation gauge (Ott Pluvio, Kempten, Germany) at the MET station (Fig. 1). Additionally, to have gap-free precipitation and potential evapotranspiration (PET) products for use in quality control and filtering based on weather conditions, ancillary modeled meteorological data from the NASA North American Land Data Assimilation System (NLDAS) were downloaded as a 0.125-degree-resolution data rod at an hourly timestep for the pixel containing the station (Xia et al., 2009).

During most of the May to September fog season, stream flow was measured using a 22.5° v-notch weir installed at the outflow of the Montana flume used for year-round stream gaging. Stage in the weir was measured using a vented pressure transducer (Campbell Scientific CS450, Logan, UT, USA) connected to a CR800 data logger (Campbell Scientific Inc., Logan, UT, USA) recording at 10-minute intervals.

2.3. Data processing

Precipitation volumes recorded every 10 min at the MET meteorological station (Fig. 1) were summed to determine daily totals (mm) over each fog season (May 1 – Sept. 30) from 2020 — 2022. To account for any events caused by precipitation instead of fog drip, we removed days where the rain gauge recorded precipitation greater than one mm per day, as well as the day prior to and following the rain. Hourly measurements of leaf wetness at each study site were evaluated using the manufacturer's recommended threshold: a value greater than 280 mV reported by the LWS was considered "wet". "Fog days" were 1) those not excluded for precipitation as described above and 2) the average LWS across the four sites was ≥ 280 mV. At each site, a fog day occurred when both the canopy sensor and ground sensor were ≥ 280 mV. To understand vapor gradients driving transpiration, maximum vapor-pressure deficit was calculated for every hourly interval using temperature and relative humidity measurements collected within the canopy of each plot.

Mean daily volumetric water content (VWC, cm^3 cm^{-3}) was calculated from the 15 min soil moisture measurements within the upper 5 cm of soil — a finer temporal resolution did not provide any additional insight. To remove seasonal effects and better visualize changes in soil moisture, VWC at each site and sensor position was re-calculated as mean daily changes and as differences between hourly values and medians of the prior 24-hours.

Raw sap flow velocities were processed in SFT1 Sap Flow Tool software (v1.5, ICT International Pty Ltd, Armidale, Australia) and corrected with site-specific wood properties to account for wounding associated with sensor installation (Burgess and Downey, 2014). Sap flow velocity measurements were standardized for display and comparison between sites by representing the sap flow velocity as a percentage of the seasonal maximum recorded at each respective tree (Dawson et al., 2007; Eller et al., 2013; Burgess and Dawson, 2004). The seasonal maximum was defined as the maximum sap flow velocity between the months of May – September during each respective study year (i.e., 2020, 2021, 2022). There were numerous days in which calculations yielded negative values for sap velocities. These can indicate sap flow reversal and direct foliar uptake, as enabled by the heat ratio method which was developed with specific interest in identifying reverse sap flow in large trees (Burgess et al., 2001). However, the occurrence of negative values from the heat ratio method can also be associated with its sensitivity to probe placement errors (Iida et al. 2022; Fuchs et al., 2017; Burgess et al., 2001). Methods for estimating the offsets between probes from the ideal spacing were applied (Burgess et al., 2001). While this spacing-estimation method is ideally conducted by severing stems from roots to ensure that sap flow is zero (Burgess et al., 2001), we approximated that method by assuming zero sap flow occurs when 1) it had rained at least 5 mm on both that day and the prior day, 2) the time was between 2:00 and 5:00 am so there was no solar radiation, and 3) the NLDAS PET ≤ 0; those conditions also mitigated the likelihood of reverse sap flow because soils would be wet. We found evidence that suggested there were errors due to misalignment (not shown), which did not influence relativistic interpretations (i.e., the rank from higher to lower was accurate), but it did influence the true 'zero' position, and thus analyzing the frequency of negative sap flow events was sensitive to those corrections and assumptions made when applying those corrections. Rather than propagating errors through attempting to correct the data, we restricted our interpretations of the sap-flow data to variations for each tree and their association compared to occurrences of fog and other meteorological conditions. Those values were also standardized by either dividing sap-flow values by seasonal maxima, or by analyzing them as anomalies from a 6-day running median (omitting those values when daily rainfall exceeded 1 mm). Those hourly values were then aggregated to a daily temporal resolution to remove diurnal fluctuations and focus on differences between days with fog and days without.

For streamflow, 10-minute stage data were reviewed alongside manual depth measurements and adjusted for anomalies due to debris in the v-notch or other equipment issues. Stage was converted to discharge using a standard rating equation (Eq. (1); Leopold and Stevens, 1978).

$$Q = 0.497\ x\ H^{5/2} \tag{1}$$

Where Q was mean daily discharge in ft^3 s^{-1} and H was stage height in ft; Q was subsequently converted to m^3 s^{-1} and normalized by dividing by the area of the sub-watershed and converted to mm. Change in daily discharge (mm) for each day was calculated using Eqn. (2).

$$\Delta Q_i = Q_i - Q_{i-1} \tag{2}$$

Where Q_i was mean daily discharge in mm for day i. Omitting days with rain and the day before and after rain as described above as well as days when ZIE flow was zero, an unpaired one-sided t-test (R Core Team, version 4.4.1, 2024) was used to determine if mean discharge declines were lower on "fog days".

3. Results

3.1. Climate and fog presence

During the 3-year study period, precipitation was below normal and severe drought spanned 2020 and 2021 (Keppeler et al., 2024). Precipitation during water years (1 October – 30 September) 2020, 2021, and 2022 totaled 660 mm, 601 mm, and 977 mm or approximately 59 %, 49 %, and 85 % of the long-term (60-year) average, respectively. Fog season (May through September) precipitation varied as well, totaling 77, 62, and 142 mm for 2020, 2021, and 2022. During these summer months, several small precipitation events occurred, predominantly early or late in the fog season. Fog frequency was highest during summer 2020 — 2/3 of the days between May 1 – Sept. 30 met our definition of fog days ($n = 103$; Fig. 3).

Fog presence varied across study sites over the fog seasons, as estimated by using the degree of leaf wetness. Both shoulder hillslope positions recorded the highest degrees of fog presence, regardless of

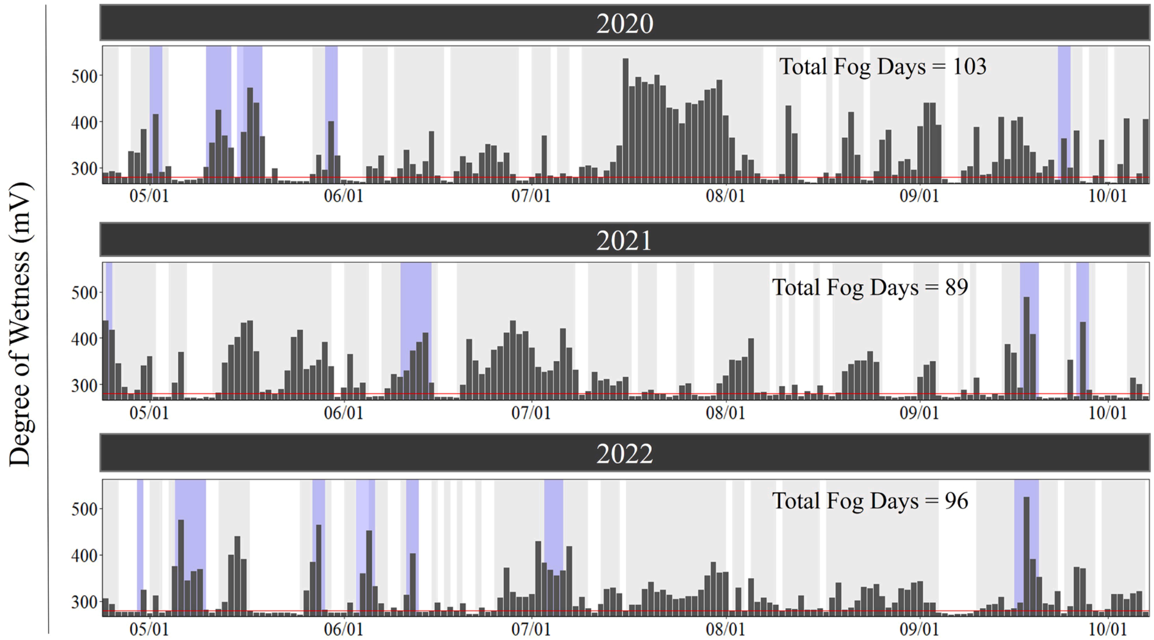

Fig. 3. Daily LWS measurement averaged across all sites, used to determine number of "fog days" per season. Red line at 280 mV indicates water deposition on the LWS. Blue background shading indicates precipitation greater than one mm; grey shading indicates fog day.

harvest treatment (Fig. 4). Fog days, defined by an increase in LWS readings >280 mV on average across all four sites, typically involved increases in LWS across all of the sites. Leaf wetness intensities during fog events were similar to those of rain events. Interestingly, the leaf-wetness-sensor values of the shoulder sites were both especially prominent in 2020, whereas only the forested shoulder site far exceeded the others in 2021, and then the fog events during 2022 yielded lower maximum LWS intensities for the forested shoulder site.

Analysis of Variance (ANOVA) tests between the topographic positions suggest that the shoulder sites had higher mean LWS values across all three study years ($p < 0.001$), with year interacting with topographic effects of fog ($p = 0.011$) (Fig. 5). There were no statistically significant differences in LWS between the forested and harvested sites ($p = 0.605$). Overall, the forested shoulder site had the highest mean LWS (and the greatest variability) across the three study years, while the ridges had the lowest mean LWS (Table 2).

General diurnal trends in leaf wetness indicated that fog or the moisture from fog was present in the evening as PAR decreased and dissipated as PAR increased over the course of the next day (Fig. 6). The vapor pressure deficit (VPD) also followed a diurnal trend that was similar to that of solar radiation, generally reaching zero when leaf wetness, or fog, was at its peak.

3.2. Soil moisture responses to fog

Soil moisture variations were positively correlated with fog days, although rain was more influential across the growing season (Fig. 7 and Fig. 8). While surficial soils displayed observable declines in VWC during periods without fog, the decline in VWC became more gradual and began to stabilize when fog persisted for several days. For examples, see the decreases in soil moisture that occurred on Aug. 15–16, 2020, and Sept. 6–7, 2022 (Fig. 6 and Fig. 7). Comparisons of means by 2-sample t-

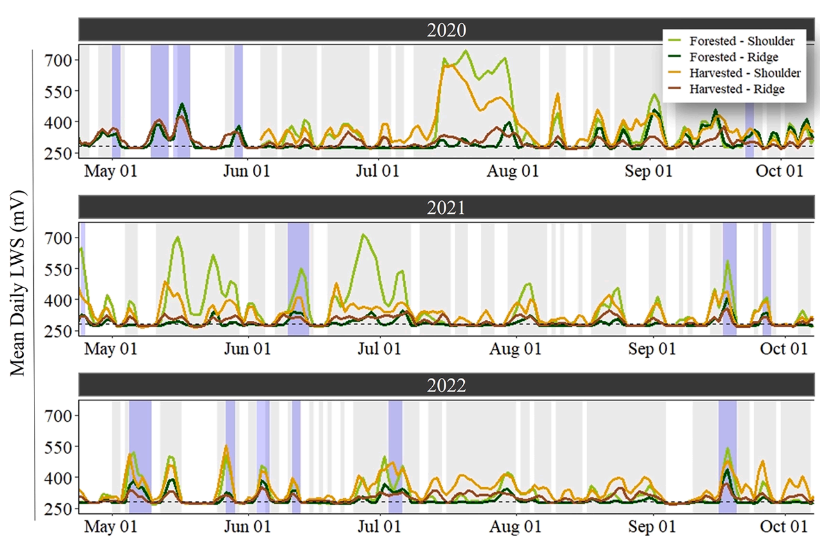

Fig. 4. Leaf wetness intensities over the three fog seasons (2020 – 2022). Days with mean LWS values above 280 mV (fog presence) are indicated with light grey shading. Blue shading shows days with rainfall > 1 mm.

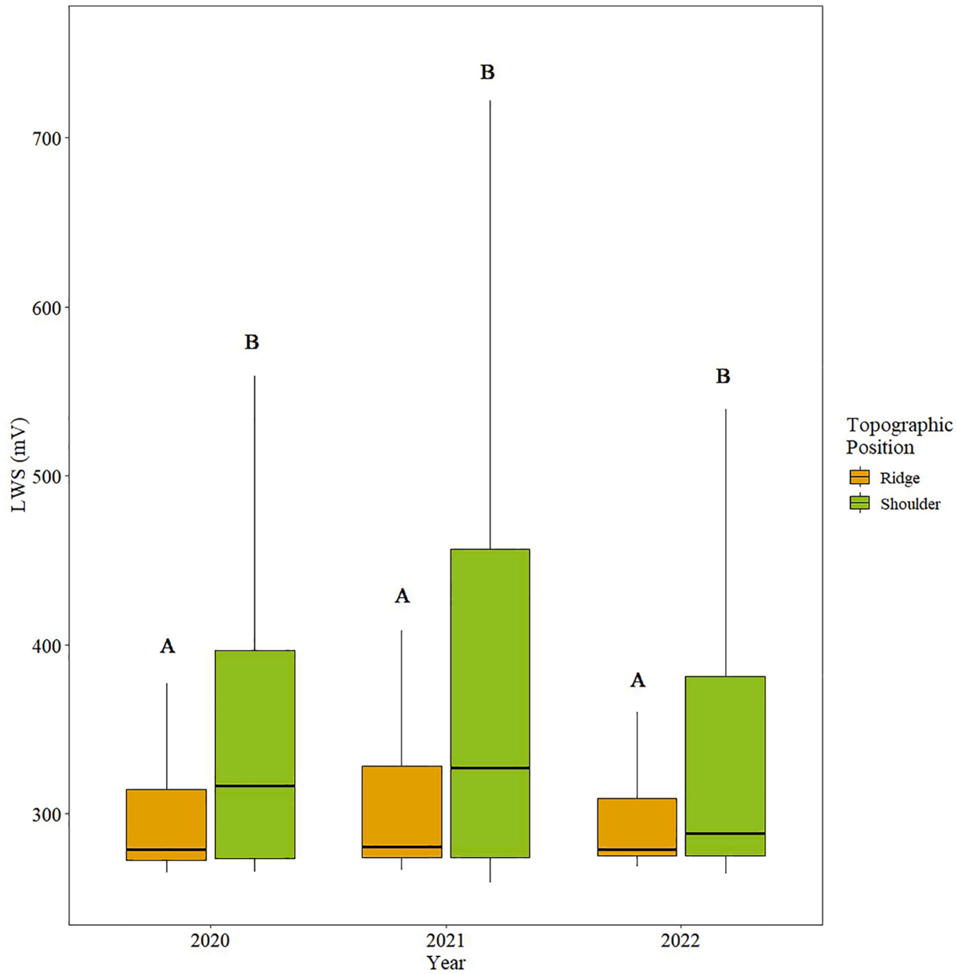

Fig. 5. Mean leaf wetness sensor values (mV) for each topographic position for each study year during the summer fog season. Letters denote significant differences in groups ($p < 0.05$) during each year as determined by Tukey's HSD.

Table 2
Mean daily leaf wetness values (LWS, mV) during fog days and standard deviation (SD) from the foggy season (May – Sep) 2020 – 2022 for the four study sites.

Site	Mean LWS (mV)	SD	n
Forested Shoulder	357	122	864
Forested Ridge	304	58	898
Harvested Shoulder	361	100	864
Harvested Ridge	305	38	898

tests showed that change in daily VWC (ΔVWC) was more negative (i.e., VWC decreased more) on non-foggy days than on foggy days at all sites (Table 3).

Soil moisture varied among and within sites across the fog seasons. The harvested ridge site had the overall lowest VWC of surface soil at all positions during the three sampling years, frequently showing values of zero. Because these sensors reported positive VWC at the beginning of the dry season (summer), observations of zero were assumed to indicate that the soils were drier than the sensors can detect (using standard calibration), rather than the sensor malfunctioning. Fig. 7 shows that VWC of surface soils (5 cm) was often highest near the bole, especially at the sites located on the hillslope shoulder. In 2020, soil moisture at the canopy drip edge was highest in the forested sites (i.e., both shoulder and ridge hillslope positions). However, in 2021 and 2022, the forested ridge site was wetter at this position than the other sites; both shoulder sites had similar soil VWC at this canopy drip edge position. Of the sensors positioned in nearby openings, the forested shoulder site maintained the highest VWC at 5 cm over all sampling years (Fig. 7). This was followed by the other forested site, which typically dried to 0 % VWC mid-season (2020, 2021) or late in the summer (2022). Both the harvested sites typically dried to 0 % VWC earlier in the summer.

3.3. *Transpiration responses to fog*

The most dominant pattern in the sapflow data was the strong diel pattern in transpiration, evident at all study sites, with the lowest transpiration rates (inferred from positive sap flow) occurring at night and early mornings, and a peak or plateau occurring at midday when VPD was also highest (Fig. 9). During night times, sapflow dropped substantially in most sites and apparently approached zero when fog was present, but readers should recall (Section 2.3) that the true zero value is uncertain in this application of the Heat-Ratio Method. Fig. 9 shows a period that includes a transition from days with fog to days without fog, demonstrating a trend where days with fog had lower night-time sapflow rates than days when there was not fog; VPD values were also much higher on days without fog (Fig. 9). This association of relatively lower sap flow days with foggy days and relatively higher sap flow days with non-foggy days was highly statistically significant across all plots (Table 4). Analysis of covariance (ANCOVA) of the relationships between the leaf-wetness and sapflow anomalies from 6-day running medians, with four groupings (Forested Shoulder, Forested Ridge, Harvested Shoulder, Harvested Ridge) found the slopes to differ ($p < 0.01$) and all individual slopes were significant at $p < 0.01$ except for the

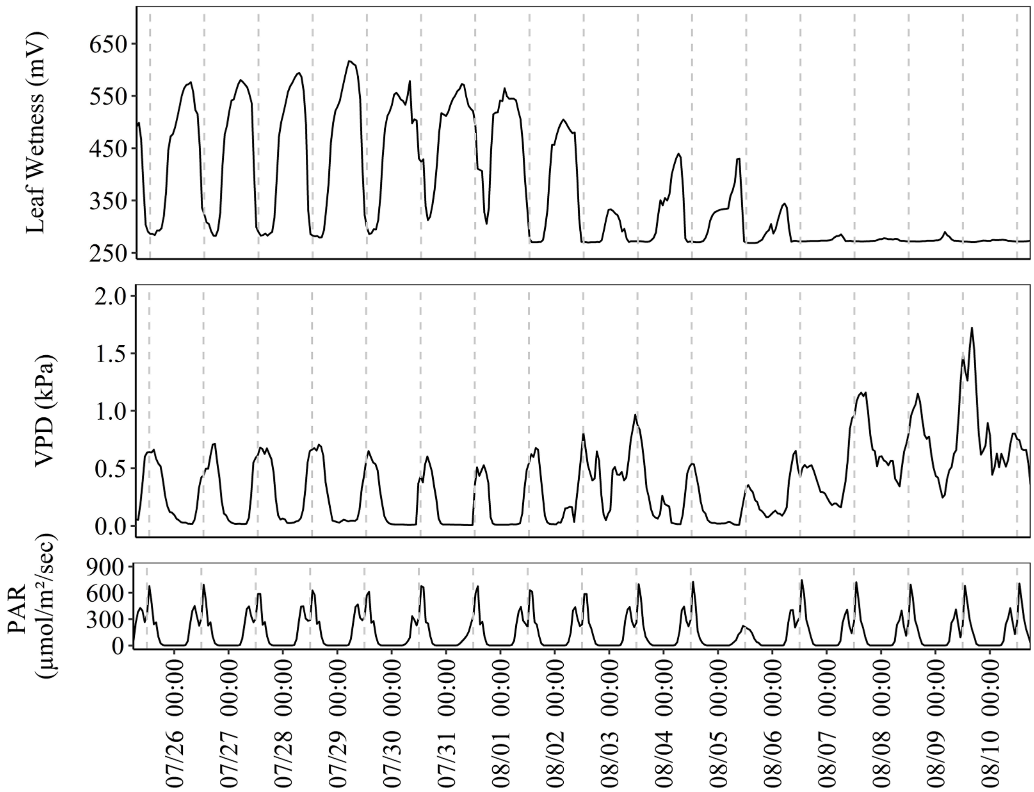

Fig. 6. Diurnal trends in leaf wetness (top), vapor pressure deficit (VPD, middle), and photosynthetically active radiation (PAR, bottom) for a period in summer 2020. A subset of data are presented to demonstrate climatic patterns when fog was present (Jul. 26 – Aug. 6) and absent (Aug. 7 – 10). Data are averages of the four study sites and dashed lines represent midday (12:00).

forested ridge site ($p = 0.06$). As with the ΔVWC data, an ANCOVA with two groupings by hillslope position was significant (Shoulder versus Ridge; $p < 0.01$), but an ANCOVA with groupings by harvesting treatment (Harvested versus Forested) did not show significant differences in slope ($p = 0.44$). These relationships between fog and daily sapflow were visually apparent across all three study seasons (Fig. 10).

3.4. Streamflow

Mean daily discharge at WIL and ZIE was below 0.17 mm day^{-1} for all three fog seasons (Fig. 11). At the beginning of each fog season, the harvested sub-watershed (ZIE, 24 ha) had similar or greater streamflow than the forested sub-watershed (WIL, 26 ha). However, as the season progressed, streamflow in the harvested sub-watershed ceased while the streamflow in the forested sub-watershed persisted through the entire fog season (Fig. 11). Discharge at the ZIE gauge ceased in early July 2021 as was typical during pre-harvest conditions, and in September of 2020 and 2022. During prolonged foggy periods occasional small increases in streamflow (generally lasting three days or less) were observed in both sub-watersheds. The most pronounced increase was observed at WIL (July 11 to 16, 2022) and totaled only 0.009 mm over the five-day period. Across all years, streamflow receded more quickly in the harvested sub-watershed irrespective of fog, while the forested sub-watershed maintained relatively constant baseflow all summer. Magnitudes of streamflow change show that both watersheds responded to fog events, and unpaired one-sided *t*-tests suggest that declines in streamflow were smaller during periods of fog inundation in both the forested and harvested watersheds in 2021 and in the aggregated 3-year data record. This was also the case in the forested watershed in 2020 (Fig. 12; Table 5).

4. Discussion

4.1. Patterns of fog at Caspar Creek

Observations of leaf wetness and vapor pressure deficit over the 2020, 2021, and 2022 fog seasons showed that fog generally rolled onto the landscape in the evening, typically several hours before solar radiation reached its minimum, and persisted into the late morning. This diurnal trend in fog presence is consistent with diurnal fog dynamics observed in other studies in coastal California (Fischer and Still, 2007; Hiatt et al., 2012; Rastogi et al., 2016; Keppeler 2007). While we used a midnight-to-midnight approach to differentiate a “fog day”, the observed evening-morning fog patterns suggest that a noon-to-noon “day” may be a more appropriate interval in future analyses.

An average of 62 % of the days in these three fog seasons were fog days. In 1971, Azevedo and Morgan (1974) recorded 43 – 61 % fog days from July 19 – September 2 in one coastal and one inland site in the Eel River Valley in northern California. A previous CCEW study reported fog presence during about one-third of the days from June through September days during 1998 and 1999; fog drip was measurable on 24 and 29 fog events in each year, respectively (Keppeler, 2007). In 2010, Johnstone and Dawson suggested that fog frequency in coastal California may be declining — they reported summertime fog frequency was 62 % in 1950, a low of 27 % in 1997, and a partial recovery from 2000 – 2010 (to 44 %). Our three-year dataset suggests that summertime fog frequency at Caspar Creek was comparable to the mid-twentieth century ranges in these prior studies. However, the higher fog frequency observed in our study may result from dew moisture on the leaf wetness sensors being indistinguishable from fog.

4.2. The importance of fog in reducing soil drying

We found that air temperature decreased, and relative humidity

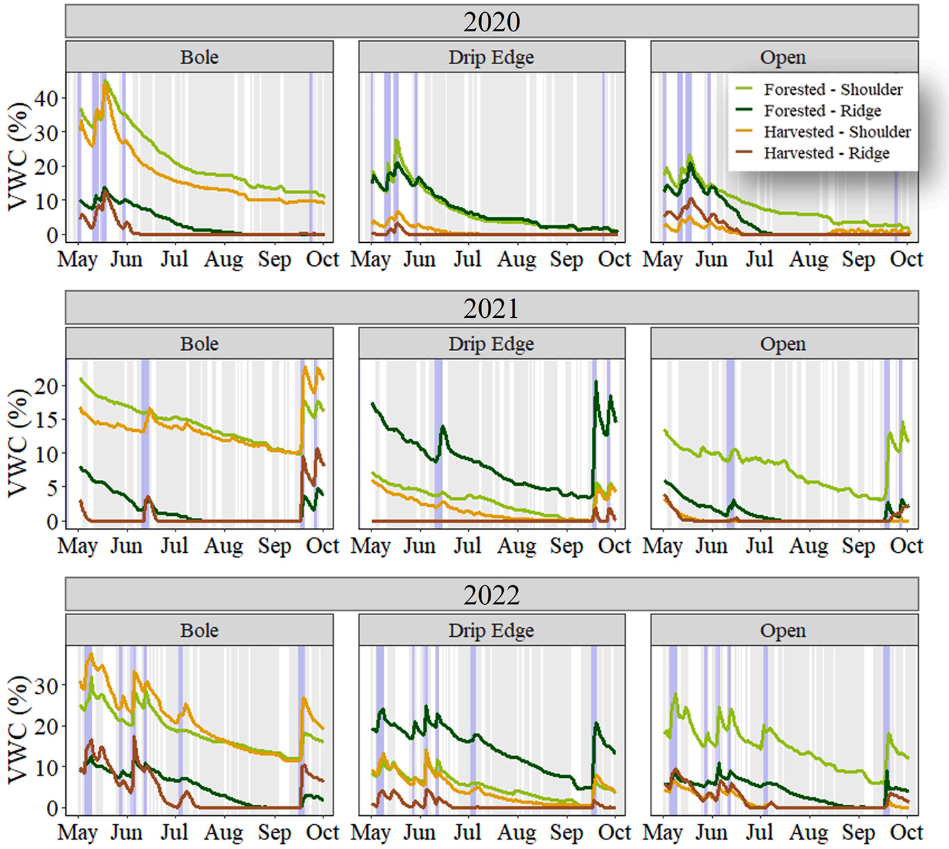

Fig. 7. Surface soil moisture (5 cm) for the 2020–2022 fog seasons at three positions: near the bole of coast redwood tree (left), at the canopy drip edge (middle), and in a nearby opening (right). The openings at the "forested" sites still contain some overhead canopy. Days with fog presence are indicated with light grey shading. Blue shading shows days with rainfall > 1 mm.

increased during fog presence, which decreased or eliminated the VPD, potentially cascading to cause the observed decreases in transpiration and soil moisture withdrawal. While VWC generally declined throughout the summer as soils dried, regardless of fog occurrence, those declines were smaller during or following foggy days. Even if fog and fog-free days had statistically distinct changes in VWC, these differences were small. Thus, daily changes in VWC may reflect reductions in transpiration (Table 4) more than they reflect fog drip adding moisture to soils. This result is consistent with Keppeler (2007), who reported a maximum single-day fog drip accumulation at CCEW of 18 mm—an amount unlikely to enhance soil moisture beyond the upper several centimeters of the litter and soil profile. Overall, surficial soils were wettest near the boles of *S. sempervirens* trees at the two shoulder sites, which also reported the highest intensities of leaf wetness. A reduction of VPD and transpiration by fog and associated reduction in soil desiccation are great ecohydrological benefits during periods of drought in California (Burgess and Dawson, 2004; Fischer et al., 2009; Carbone et al., 2011) and other global fog-inundated ecosystems (Hildebrandt et al., 2007; Ritter et al., 2008).

Although surficial soil moisture (5 cm depth) was not always supplemented by fog events, it increased by an average of 1–2 % VWC in response to small, infrequent summer rain events (Figs. 7 and 8). During our study period, some larger rain events (21 – 58 mm) did occur in June and September, resulting in VWC increases >2 %. Fog drip can contribute large depths of water to California coast redwood forests. Although we did not directly quantify the volumetric water input of fog drip to our soils, past studies have recorded 175 to > 900 mm of water per fog season in northern or southern California (Azevedo and Morgan, 1974; Fischer and Still, 2007; Fischer et al., 2009; Sawaske and Freyberg, 2015) although past measured quantities were <100 mm at Caspar Creek (Keppeler, 2007). In the Santa Cruz Mountains, fog drip has been shown to infiltrate to depths of 23 cm during the dry summer months (Sawaske and Freyberg, 2015). While the overstory vegetation in the Santa Cruz study (*S. sempervirens* and *P. menziesii*) was similar to our study site, fog drip was an order of magnitude greater than what was previously measured at Caspar Creek (Keppeler, 2007). However, it should be noted that the aforementioned studies mention that fog drip is highly variable and challenging to accurately quantify.

4.3. Influence of fog on overstory transpiration

Transpiration rates (as captured by sap flow velocities) declined with fog presence over the 2020 – 2022 fog seasons. Our results are similar to those found in other northern California ecosystems, which suggest that the foggy season is important for suppressing plant-water-use and soil water drawdown as opposed to contributing direct ecosystem water inputs (Ewing et al., 2009; Chung et al., 2017). Physiologically, there are many explanations for fog reducing transpiration rates: for example, fog effects on reduced VPD, diffuse light, foliar uptake and reverse sap-flow, or leaf wetness directly impeding stomatal gas exchange (e.g., Dawson and Goldsmith, 2018; Baguskas et al., 2021). Given that VPD was observed to decline with fog, and relationships between VPD and transpiration are of widespread importance (Liu et al., 2020), this is likely a major explanation of why transpiration reduced with fog. An additional explanation for the reduced transpiration during fog events may be changes in diffuse PAR that occur during fog events. For instance, Baguskas et al. (2021) found that PAR and ET decreased during fog events over strawberry fields in Central California. Light Use Efficiency (LUE) and Water Use Efficiency (WUE), however, increased during fog events due to an increase in the fraction of diffuse PAR, while Gross

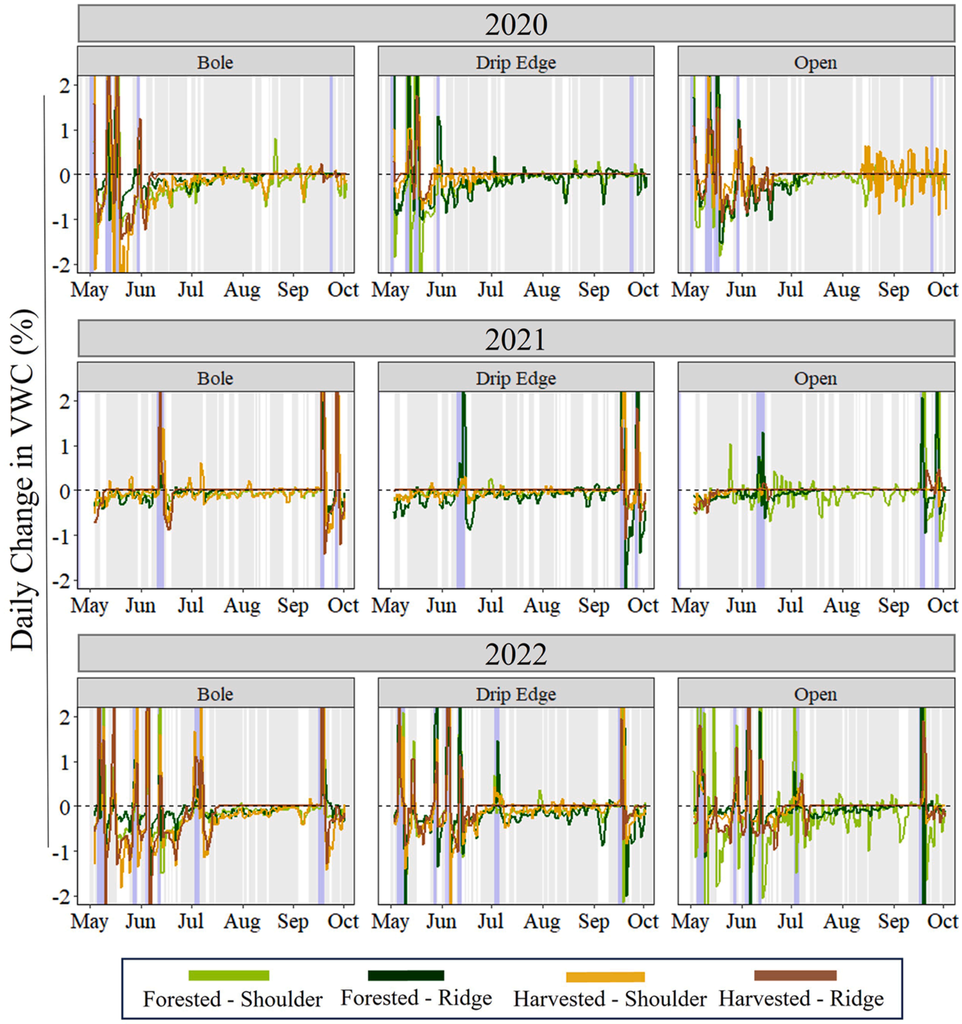

Fig. 8. Daily changes in mean daily VWC (%) of surface soils (5 cm) at different positions relative to the study tree: near the bole (left), at the canopy drip edge (middle), and in a nearby opening (right). Graphs are centered around the horizontal zero line; increases from the previous day's soil moisture plot above the line, while decreases plot below the line. Days with fog presence are indicated with light grey shading. Blue shading shows days with rainfall > 1mm.

Table 3
Mean change (± standard error, SE) in soil moisture (volumetric water content, ΔVWC) during days with and without fog, p-values for T-tests for difference in VWC between days with and without fog, and correlation coefficients between unlagged and 1-day lagged changes in VWC and leaf wetness.

Site	ΔVWC, days with fog (%, mean ± SE) (%, mean ± SE)	ΔVWC, days without fog (%, mean ± SE)	p-value from 2-sided t-test	*Pearson correlation coefficient* ΔVWC vs Leaf Wetness (no lag)	*Pearson correlation coefficient* ΔVWC vs Leaf Wetness (1-day lag)
Forested Shoulder[1]	−0.02. ±0.01	−0.15. ±0.01	< 0.001	0.53	0.47
Forested Ridge[2]	0.20. ±0.09	−0.20. ±0.02	< 0.001	0.6	0.36
Harvested[3] Shoulder	−0.04. ±0.01	−0.13. ±0.02	< 0.001	0.14	0.27
Harvested[4] Ridge	0.05. ±0.05	−0.12. ±0.02	0.002	0.26	0.42

[1] using data from May-Sept 2021 for the Forested Shoulder site.
[2] using data from May-Sept 2020 and 2021 for the Forested Ridge site.
[3] using data from June-Sept 2020 and 2021 for the Harvested Shoulder site.
[4] using data from May-Sept 2020 and 2021 for the Forested Ridge site.

Primary Productivity (GPP) remained unchanged between clear sky and foggy days (Berry and Goldsmith 2020; Baguskas et al. 2021). If these results are transferrable to our sites, this suggests that a reduction in transpiration may not correlate to reduced photosynthesis, which could be a factor contributing to the high productivity of coast redwood trees.

Others have found that redwood transpiration rates can be high on dry nights, up to 40 % of maximum transpiration (Burgess and Dawson, 2004), with fog dramatically reducing those night-time fluxes. However, challenges inherent to the HRM method precluded us from clearly characterizing night-time fluxes. For example, the forested-ridge sap flux values in Fig. 9 show high values at night, but we suspect those values reflect an error in sensor positioning such that the true zero-flux value is reading as ~30 % of maximum; comparison of that tree to the other three further supports this inference. Correction methods (Burgess et al., 2001) require destructive methods that are not feasible here. We also opted to not apply ad-hoc corrections to mitigate the consistently high nighttime fluxes in that tree, because there was no obvious value to use as a benchmark (because reverse sap flow is likely). Thus, we cannot infer the actual value of night-time transpiration in this study, and instead relied on interpretation of trends and anomalies from running means, which are standardized and thus only require an assumption of relativistic accuracy.

Regarding other potential effects of fog on transpiration, one of the sites (the forested shoulder site) frequently had leaf wetness intensities

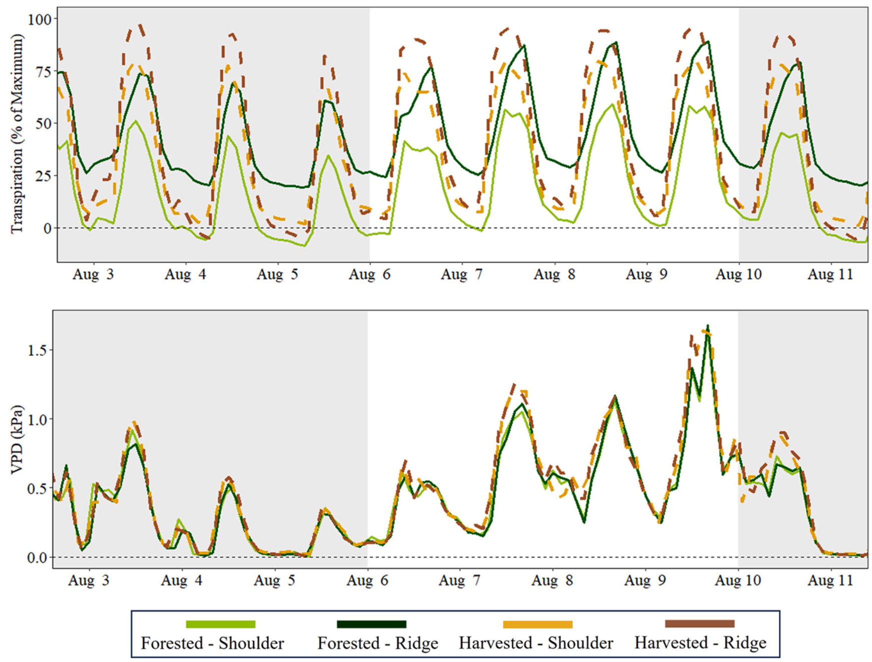

Fig. 9. Example diurnal trends in transpiration (top) and VPD (bottom) over periods with and without fog in August 2020. Transpiration refers to sap flow velocity values displayed as percentage of tree-specific seasonal maximum. VPD (kPa) is the hourly maximum at each site. Background shading indicates periods of leaf wetness (fog presence) at all sites. This subset of data was chosen to display typical patterns of transpiration and VPD during fog presence and absence.

Table 4
Daily sap flow anomalies (6-day running medians) for days with and without fog and statistical results from 2-sided T-test.

Site	Sap flow anomaly, days with fog (%, mean ± SE)	Sap flow anomaly, days without fog (%, mean ± SE)	p-value of 2-sided t-test
Forested Shoulder[1]	−9.8 ± 3.0	+12.0 ± 2.4	<0.001
Forested Ridge[2]	−11.3 ± 2.4	+4.0 ± 1.3	<0.001
Harvested[3] Shoulder	−6.0 ± 1.5	+8.1 ± 1.8	<0.001
Harvested[4] Ridge	−11.9 ± 4.7	+6.6 ± 3.0	0.003

[1] using data from May-Sept 2021 for the Forested Shoulder site.
[2] using data from May-Sept 2020 and 2021 for the Forested Ridge site.
[3] using data from June-Sept 2020 and 2021 for the Harvested Shoulder site.
[4] using data from May-Sept 2020 and 2021 for the Forested Ridge site.

exceeding common values reported in other studies (e.g., Goldsmith et al. 2012). Excessive deposition of fog water on foliage can suppress transpiration and thereby decrease photosynthesis and reduce growth. However, such conditions may also allow *S. sempervirens* to utilize fog water via direct foliar uptake as well as stored bark water (Burgess and Dawson, 2004; Simonin et al.; 2009; Earles et al., 2015), albeit this typically only equates to a small fraction of daily water use; for example, instantaneous reverse flow rates of 5–7 % of the maximum transpiration have been reported for *S. sempervirens* (Burgess and Dawson, 2004). Although the uncertainty in these heat-ratio method sap flow values precludes precisely identifying instances of sap flow reversal, it is likely that many of the especially negative values shown (e.g., Fig. 10) were indeed reverse sap flow at Caspar Creek. Additional studies on hydraulics, leaf gas-exchange, and photosynthetic capacity of coast redwood during fog events will help clarify the impacts of fog on coast redwood physiology and growth.

4.4. Fog variation across topography and vegetation density

Although evidence of fog drip and transpiration reduction was present at all sites over the three fog seasons, responses varied in timing and magnitude across the four study sites. Following most fog events, leaf wetness was higher at the hillslope shoulder sites than at ridge tops (Table 2). While the elevation difference between shoulder and ridge sites was relatively small in each watershed (22 m; Table 1), we found significant differences between our topographic positions that were consistent across all years (Fig. 5). In a study approximately 200 km south of our sites in the Santa Cruz Mountains in Coastal California, Chung et al. (2017) found that leaf wetness was highest at mid-elevation sites and then reduced with elevation as the fog bank proceeded into the forest interior. They had a similar elevation gradient to our study (15 m) but used a spatial averaging scheme to upscale their results to the watershed scale. Because of the similarities in ridge LWS between our forest and harvested sites, it is possible that the topographic controls outweigh the forest density controls at this site. We suggest additional study sites would help to fully discern the differences between topographic and forest density controls on fog deposition.

Fog is spatially and temporally heterogeneous across forested mountainous terrain (e.g., Ewing et al., 2009; Sawaske and Freyberg, 2015; Chung et al., 2017; Ball and Tzanopoulos, 2020; Hůnová et al. 2021). Previous analyses of fog and low clouds along the northern California coast show that terrain oriented to the prevailing northwest winds will likely have the greatest amount of fog and low cloud cover (Torregrosa et al., 2016). Both shoulder sites had more northerly aspects (351 – 357°) compared to the more westerly aspects (288 – 294°) of the two ridge sites. In a study in the Santa Cruz Islands in southern California, Fischer et al. (2009) also hypothesized that northern aspects would experience the most fog. Ultimately, the role of aspect in controlling fog in complex forested terrain can be difficult to disentangle, especially due to the larger driving factors of elevation, distance from coast, and vegetation (Hůnová et al. 2020). In our study, the harvested shoulder site had fog deposition associated with northwest and easterly wind directions, and the forested shoulder site received most winds from the northwest (Petreshen 2021). Therefore, based on aspect and

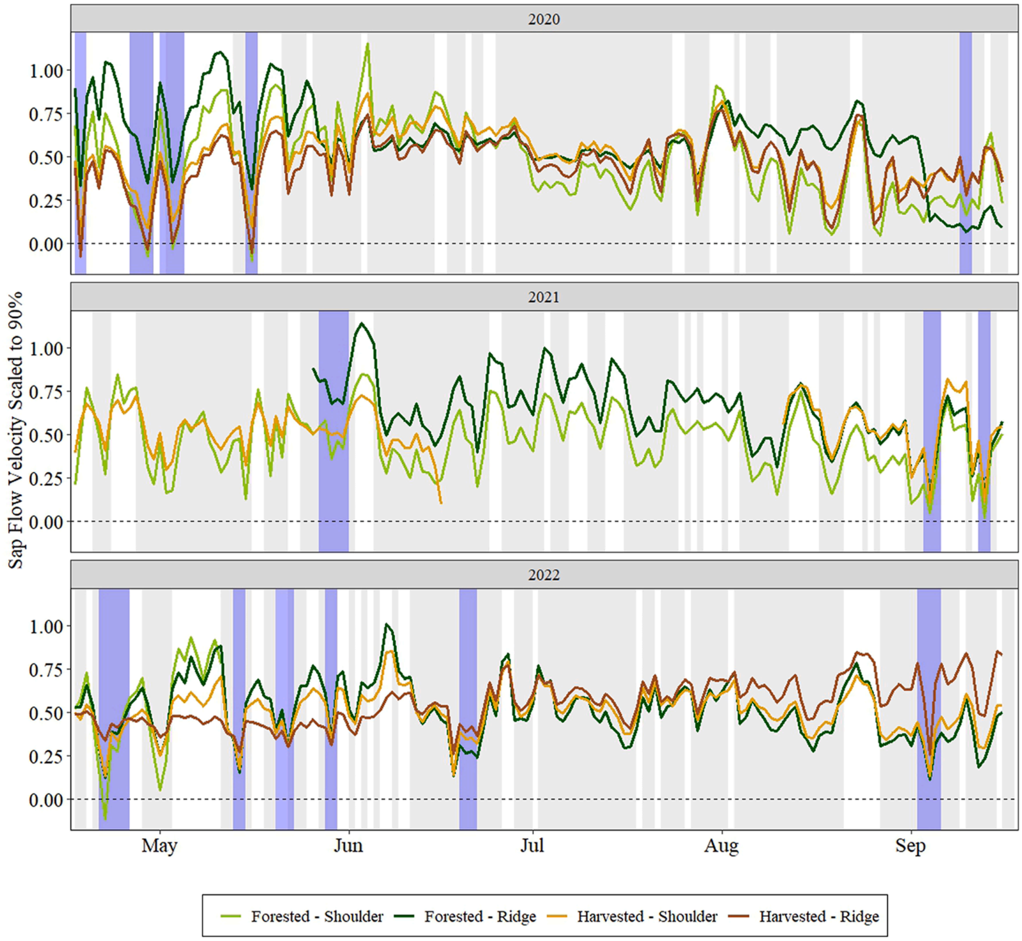

Fig. 10. Mean daily sapflow velocity of each study tree over three fog seasons. Sap flow velocity expressed as percentage of tree-specific seasonal maximum. Background shading represents periods when fog was present at all sites for period of record (Jun 04 until Sept. 30). Blue shading shows days with rainfall > 1 mm. Data are missing for the harvested ridge tree for the 2021 season and for the harvested shoulder tree from May 2022 to July 2022.

prevailing wind direction, the shoulder sites may have had more direct exposure to fog-rich winds compared to the ridge sites, leading to greater fog deposition at the shoulder sites.

Our results suggest that there was no difference in fog magnitude between harvested and forested sites at Caspar Creek (Fig. 5; Table 2). Many studies have investigated the differences in fog across forest canopies and generally found that forest edges have greater fog occurrence than forest interiors (Ewing et al., 2009; Chung et al., 2017; Ball and Tzanopoulos, 2020). While we did not find any difference between leaf wetness magnitude between our forest and harvest sites, there is clearly a difference in leaf area between the two sites (Table 1). Thus, converting the LWS data to a metric of ecosystem water inputs would generate larger fog water contributions for the forested site relative to the harvested site due to its higher stand density. Unpublished throughfall data collected from our sites at Caspar Creek suggest that the forested sites have higher interception than the harvested sites, and results from a previous study at Caspar Creek demonstrate that harvesting increases net precipitation by 20–30 % in clearcut versus unharvested stands (Reid and Lewis, 2009).

In addition to terrain differences, species composition varied slightly across our sites, which may have contributed to variations in fog drip and ecosystem responses. While *S. sempervirens* dominates the overstory at Caspar Creek, the forested shoulder site had a greater proportion of *P. menziesii* (Table 1). Field observations over the 2020 fog season indicated significant fog drip under *P. menziesii* resulting in puddling along roads and wetting herbaceous understory vegetation including *Oxalis* — this was not typically observed under *S. sempervirens* canopies. The higher proportion of *P. menziesii* at the forested shoulder site may explain their higher rates of fog deposition recorded by leaf wetness and soil moisture sensors.

Among our study sites, the harvested ridge site had the lowest fog-season surficial (5 cm) soil moisture, which was consistent with pre-harvest soil moisture conditions (Dymond et al., 2021b), but still maintained the highest peaks in daily transpiration late into the fog season. A previous study of fog drip at Caspar Creek suggested that clearings can receive similar amounts of fog drip as full-canopy sites (Keppeler, 2007), so the fog drip inputs in the harvested sites were likely similar to the forested sites; indeed, the harvesting seemed to be less influential on fog deposition than hillslope position. In studies at other locations, it has been shown that soils in clearings affected by fog drip are significantly drier than soils under canopies (Ataroff and Rada, 2000; Fischer et al., 2009). Harvesting has been shown to increase individual tree transpiration, with variable effects on soil evaporation (e.g., Bréda et al., 1995; del Campo et al., 2022; and many others). Thus, differences in overall transpiration rates between the forested and harvested sites were likely due to higher light availability and reduced competition from surrounding vegetation in the harvested site.

4.5. Fog and streamflow

Our results indicate modest reductions in mean daily streamflow recession during periods of fog (Fig. 12; Table 5). However, statistically significant differences between fog day and clear day declines were not detected in the forested or harvested watershed during the 2022 fog

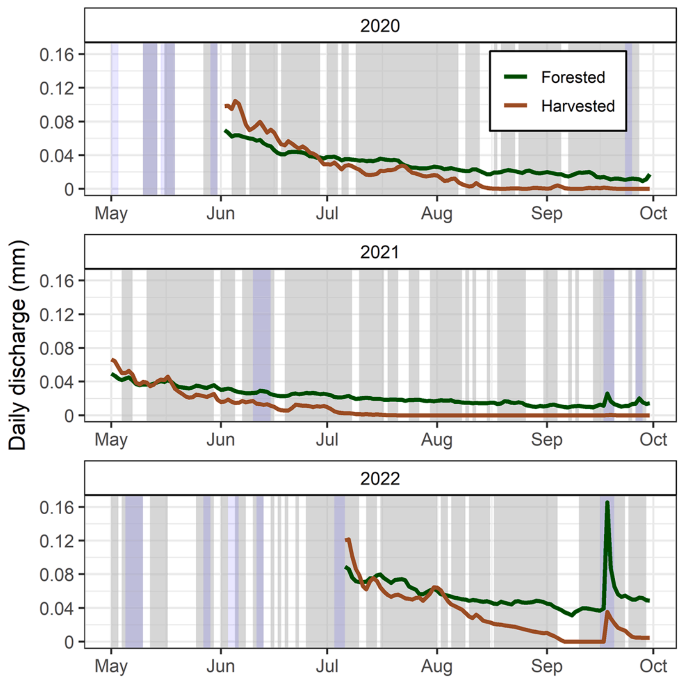

Fig. 11. Mean daily discharge in the forested and harvested sub-watersheds over three fog seasons. Light grey background shading represents periods when fog was present at all sites, blue indicates rainfall.

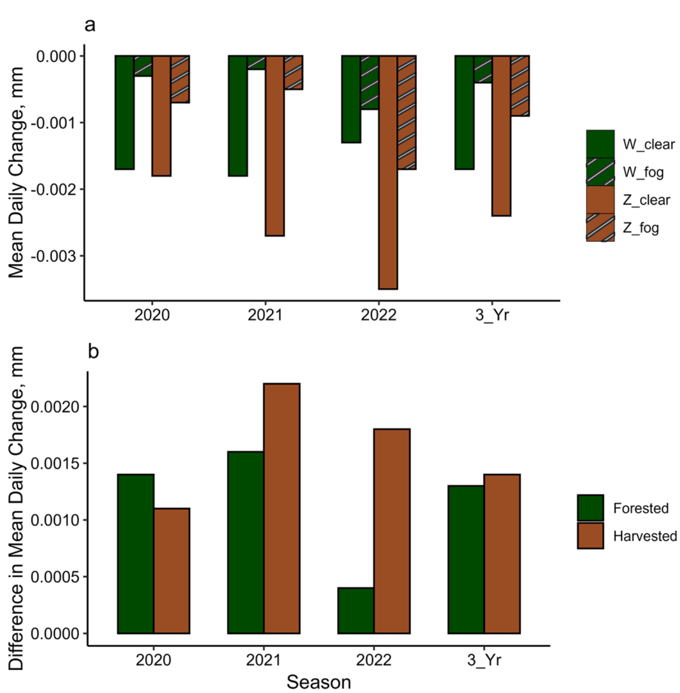

Fig. 12. (a) Mean daily change in streamflow in the forested (WIL, "W") and harvested (ZIE, "Z") watersheds in the presence and absence of fog across three fog seasons and aggregate 3-year data. (b) Difference between mean daily streamflow change in the presence and absence of fog across three seasons and aggregated 3-year data for the forested watershed and harvested watershed.

season. This result may reflect variations in hydrological processes in either annual or sub-monthly conditions. For example, 2022 was wetter, with higher baseflows than the two prior years in this study, and September 2022 flows increased significantly in response to the unusual 65 mm rain event that occurred mid-month. It appears that the streamflow response to fog was most evident during 2020 and 2021, which were extreme drought years (Keppeler et al., 2024). This suggests a decline in fog frequency resulting from a warmer climate (Johnstone and Dawson, 2010; Werner et al., 2022), may disproportionately affect drought-year streamflow, and hence water supplies, in the coast redwood region.

Although the greatest difference in transpiration between clear and foggy nights occurred at the harvested sites, the mean daily streamflow declines after clear and foggy nights did not vary between the harvested and forested sites. The trend across the three study years suggests that as the harvested stand regrew, declines in streamflow during fog-free days intensified (Fig. 12). We hypothesize that continued monitoring will show that this trend will continue as the stand regrows and transpiration demands increase.

5. Conclusions

Observations of leaf wetness, soil moisture, sap flow, and streamflow in two sub-watersheds of the South Fork of Caspar Creek indicated fog presence and ecosystem responses to fog over the 2020–2022 fog seasons. Despite the small sample size of our study, we found a clear relationship between fog presence and lower VPD, reduced transpiration, lower drying rates of forest soils, and reduced rates of streamflow recession during the summer fog season. Fog reduced transpiration rates of *S. sempervirens* trees in both harvested and unharvested sites, but the greatest difference in transpiration between clear and foggy nights occurred at the harvested sites. Variation in fog deposition as inferred from soil volumetric water content was observed across all four sites and may have been driven by site-specific characteristics such as hillslope aspect and species composition. Some observations indicated higher fog drip under *P. menziesii* as compared to *S. sempervirens*.

We found no difference in fog magnitude, VPD, or surficial soil moisture between the forested and harvested sites during fog events. While timber harvest can have substantial impacts on water balance components in coastal California climates (e.g., Keppeler and Ziemer, 1990), our results suggest that topographic controls had a higher control on fog interception than forest density. While our results show that individual coast redwood trees may be able to intercept and utilize fog, we did not explicitly measure throughfall and thus our results should not be interpreted as impacts of harvesting on catchment-scale hydrology.

Our results suggest that the effects of climate change on fog presence and intensity are important areas of continued study. A decline in fog presence as suggested by earlier studies (Johnstone and Dawson, 2010; Werner et al., 2022) may subject coastal California forests to greater drought stress and reduced biomass production (Sillett et al., 2022). Adaptation to reduced fog inputs may lead to different stand conditions across aspects, with the least effect in areas where aspect aligns with dominant wind directions during fog events. We demonstrate the need to continue investigating fog dynamics in the coast redwood region, including 1) the effect of climate change on fog dynamics, 2) potential variations in fog deposition beneath *S. sempervirens* and *P. menziesii* canopies, and 3) the ecohydrological impacts of fog. Our results suggest that the presence of fog provides ecohydrological benefits to ecosystems in coastal California, primarily by relieving water stress during periods of seasonal drought.

CRediT authorship contribution statement

Julia Petreshen: Writing – review & editing, Writing – original draft, Visualization, Methodology, Investigation, Formal analysis, Data curation, Conceptualization. **Salli F. Dymond:** Writing – review & editing, Writing – original draft, Visualization, Supervision, Resources, Project administration, Methodology, Investigation, Funding acquisition, Formal analysis, Conceptualization. **Elizabeth T. Keppeler:** Writing – review & editing, Writing – original draft, Visualization, Methodology, Formal analysis. **Scott T. Allen:** Writing – review &

Table 5
Mean daily change in streamflow for days with and without fog and statistical results from a 1-sided *t*-test. Bold p-values indicate significantly smaller mean daily declines during fog days (α = 0.05).

Year	Forested, days with fog (mm, mean ± SE)	Forested, days without fog (mm, mean ± SE)	p-value	Harvested, days with fog (mm, mean ± SE)	Harvested, days without fog (mm, mean ± SE)	p-value
2020	−0003 0003 ± 0.0001	−0.0017 ± 0.0003	**< 0.001**	−0.0007 ± 0.0003	−0.0018 ± 0.0009	0.135
2021	−0.0002 ± 0.0001	−0.0018 ± 0.0004	**0.002**	−0.0005 ± 0.0003	−0.0027 ± 0.0011	**0.038**
2022	−0.0008 ± 0.0003	−0.0013 ± 0.0005	0.244	−0.0017 ± 0.0005	−0.0035 ± 0.0024	0.251
3-yr	−0.0004 ± 0.0001	−0.0017 ± 0.0002	**< 0.001**	−0.0009 ± 0.0002	−0.0024 ± 0.0007	**0.026**

editing, Writing – original draft, Visualization, Formal analysis. **Joseph W. Wagenbrenner:** Writing – review & editing, Visualization, Resources, Project administration, Methodology, Funding acquisition, Formal analysis, Conceptualization.

Declaration of competing interest

The authors declare the following financial interests/personal relationships which may be considered as potential competing interests:

Salli Dymond reports financial support was provided by National Science Foundation. Salli Dymond reports financial support was provided by USDA Forest Service Pacific Southwest Research Station. Joseph Wagenbrenner reports was provided by California Department of Forestry and Fire Protection. If there are other authors, they declare that they have no known competing financial interests or personal relationships that could have appeared to influence the work reported in this paper.

Acknowledgements

Funding and support for this project was provided by the California Department of Forestry and Fire Protection, the USDA Forest Service Pacific Southwest Research Station (PSW), and the National Science Foundation (NSF) (NSF-EAR-1807165). We especially thank Brian Storms, Megan Arnold, Jayme Seehafer, and the Caspar Creek Watershed Experiment field team for data collection and technical assistance.

Data availability

Data will be made available on request.

References

Arkley, R.J., 1981. Soil moisture use by mixed conifer forest in a summer-dry climate. Soil Sci. Soc. Am. J. 45 (2), 423–427.
Ataroff, M., Rada, F., 2000. Deforestation impact on water dynamics in a Venezuelan Andean cloud forest. Ambio 29 (7), 440–444. https://doi.org/10.1579/0044-7447-29.7.440.
Azevedo, J., Morgan, D.L., 1974. Fog precipitation in coastal California forests. Ecology 55 (5), 1135–1141.
Baguskas, S.A., Oliphant, A.J., Clemesha, R.E.S., Loik, M.E., 2021. Water and light-use efficiency are enhanced under summer coastal fog in a California agricultural system. J. Geophys. Res. Biogeosci. 126. https://doi.org/10.1029/2020JG006193.
Ball, L., Tzanopoulos., 2020. Interplay between topography, fog and vegetation in the central South Arabian mountains revealed using a novel Landsat fog detection technique. Remote Sens. Ecol. Conserv. 6 (4), 498–513. https://doi.org/10.1002/rse2.151.
Barbosa, O., Marquet, P.A., Bacigalupe, L.D., Christie, D.A., Del-Val, E., Gutierrez, A.G., Armesto, J.J., 2010. Interactions among patch area, forest structure and water fluxes in a fog-inundated forest ecosystem in semi-arid Chile. Funct. Ecol. 24 (4), 909–917. https://doi.org/10.1111/j.1365-2435.2010.01697.x.
Berry, Z.C., Goldsmith, G.R., 2020. Diffuse light and wetting differentially affect tropical leaf photosynthesis. New Phytol. 1 (225), 143–153. https://doi.org/10.1111/nph.16121.
Bréda, N., Granier, A., Aussenac, G., 1995. Effects of thinning on soil and tree water relations, transpiration and growth in an oak forest (*Quercus petraea* (Matt.) Liebl.). Tree Physiol. 15 (5), 295–306. https://doi.org/10.1093/treephys/15.5.295.
Burgess, S.S., Adams, M.A., Turner, N.C., Beverly, C.R., Ong, C.K., Khan, A.A., Bleby, T. M., 2001. An improved heat pulse method to measure low and reverse rates of sap flow in woody plants. Tree Physiol. 21 (9), 589–598.
Burgess, S.S.O., Dawson, T.E., 2004. The contribution of fog to the water relations of Sequoia sempervirens (D. Don): foliar uptake and prevention of dehydration. Plant Cell Environ. 27 (8), 1023–1034. https://doi.org/10.1111/j.1365-3040.2004.01207.x.
Burgess, S.S.O., Downey, A., 2014. SFM1 Sap Flow Meter Manual. ICT International Pty Ltd.
Cafferata, P., Reid, L., 2013. Applications of Long-Term Watershed Research to Forest Management in California: 50 Years of Learning from the Caspar Creek Watershed Study. State of California, The Natural Resources Agency, Department of Forestry & Fire Protection, Sacramento, p. 110. *California Forestry Report No. 5*.
Carbone, M.S., Still, C.J., Ambrose, A.R., Dawson, T.E., Williams, A.P., Boot, C.M., Schimel, J.P., 2011. Seasonal and episodic moisture controls on plant and microbial contributions to soil respiration. Oecologia 167 (1), 265–278.
Carbone, M.S., Park Williams, A., Ambrose, A.R., Boot, C.M., Bradley, E.S., Dawson, T.E., Still, C.J., 2013. Cloud shading and fog drip influence the metabolism of a coastal pine ecosystem. Glob. Chang. Biol. 19 (2), 484–497. https://doi.org/10.1111/gcb.12054.
Cárdenas, M.F., Tobón, C., Buytaert, W., 2017. Contribution of occult precipitation to the water balance of páramo ecosystems in the Colombian Andes. Hydrol. Process. 31 (24), 4440–4449. https://doi.org/10.1002/hyp.11374.
Chung, M., Dufour, A., Pluche, R., Thompson, S., 2017. How much does dry-season fog matter? quantifying fog contributions to water balance in a coastal California watershed. Hydrol. Process. 31, 3948–3961. https://doi.org/10.1002/hyp11312.
Dawson, T.E., 1998. Fog in the California redwood forest: ecosystem inputs and use by plants. Oecologia 117 (4), 476–485.
Dawson, T.E., Burgess, S.S., Tu, K.P., Oliveira, R.S., Santiago, L.S., Fisher, J.B., Ambrose, A.R., 2007. Nighttime transpiration in woody plants from contrasting ecosystems. Tree Physiol. 27 (4), 561–575.
Dawson, T.E., Goldsmith, G.R., 2018. The value of wet leaves. New Phytol. 219, 1156–1169.
del Campo, A.D., Otuski, K., Serengil, Y., Blanco, J.A., Yousefpour, R., Wei, X., 2022. A global synthesis on the effects of thinning on hydrological processes: implications for forest management. For. Ecol. Manage. 519, 120324.
Dymond, S.F., Richardson, P.W., Webb, L.A., Keppeler, E.T., Arismendi, I., Bladon, K.D., Cafferata, P.H., Dahlke, H.E., Longstreth, D.L., Brand, P.K., Ode, P.R., Surfleet, C.G., Wagenbrenner, J.W., 2021a. A field-based experiment on the influence of stand density reduction on watershed processes at the Caspar Creek experimental watersheds in Northern California. Front. Forest. Glob. Change 4, 691732. https://doi.org/10.3389/ffgc.2021.691732.
Dymond, S.F., Wagenbrenner, J.W., Keppeler, E.T., Bladon, K.D., 2021b. Dynamic hillslope soil moisture in a Mediterranean montane watershed. Water Resour. Res. 57, e2020WR029170.
Earles, J.M., Sperling, O., Silva, L.C.R., Mcelrone, A.J., Brodersen, C.R., North, M.P., Zwieniecki, M.A., 2015. Bark water uptake promotes localized hydraulic recovery in coastal redwood crown. Plant Cell Environ. 39 (2), 320–328. https://doi.org/10.1111/pce.12612.
Eller, C.B., Lima, A.L., Oliveira, R.S., 2013. Foliar uptake of fog water and transport belowground alleviates drought effects in the cloud forest tree species, D rimys brasiliensis (W interaceae). New Phytol. 199 (1), 151–162.
Ewing, H.A., Weathers, K.C., Templer, P.H., Dawson, T.E., Firestone, M.K., Elliott, A.M., Boukili, V.K., 2009. Fog water and ecosystem function: heterogeneity in a California redwood forest. Ecosystems 12 (3), 417–433.
Fischer, D.T., Still, C.J., Ebert, C.M., Baguskas, S.A., Park Williams, A., 2016. Fog drip maintains dry season ecological function in a California coastal pine forest. Ecosphere 7 (6), e10364. https://doi.org/10.1002/ecs2.1364.
Fischer, D.T., Still, C.J., 2007. Evaluating patterns of fog water deposition and isotopic composition on the California Channel Islands. Water Resour. Res. 43 (4), 1–13. https://doi.org/10.1029/2006WR005124.
Fischer, D.T., Still, C.J., Williams, A.P., 2009. Significance of summer fog and overcast for drought stress and ecological functioning of coastal California endemic plant species. J. Biogeogr. 36 (4), 783–799. https://doi.org/10.1111/j.1365-2699.2008.02025.x.
Francis, E.J., Asner, G.P., Mach, K.J., Field, C.B., 2020. Landscape scale variation in the hydrologic niche of California coast redwood. Ecography 43 (9), 1305–1315. https://doi.org/10.1111/ecog.05080.
Fuchs, S., Leuschner, C., Link, R., Coners, H., Schuldt, B., 2017. Calibration and comparison of thermal dissipation, heat ratio and heat field deformation sap flow probes for diffuse-porous trees. Agric. For. Meteorol. 244, 151–161.
Goldsmith, G.R., Matzke, N.J., Dawson, T.E., 2012. The incidence and implications of clouds for cloud forest plant water relations. Ecol. Lett. 16 (3), 307–314. https://doi.org/10.1111/ele.12039.
Harr, R.D., 1982. Fog drip in the Bull Run municipal watershed, Oregon. Water Resour. Bull. 18 (5), 785–789.
Henry, N., 1998. Overview of the Caspar Creek Watershed study *(Ed.)*.. In: Ziemer, R.R. (Ed.), *Proceedings of the Conference on Coastal Watersheds: The Caspar Creek Story.*

Gen. Tech. Rep. PSW GTR-168. U.S. Department of Agriculture, Service, Pacific Southwest Research Station, Albany, California, p. 149.
Hiatt, C., Fernandez, D., Potter, C., 2012. Measurements of fog water deposition on the California Central Coast. Atmos. Clim. Sci. 2 (04), 525.
Hildebrandt, A., Al Aufi, M., Amerjeed, M., Shammas, M., Eltahir, E.A.B., 2007. Ecohydrology of a seasonal cloud forest in Dhofar: 1. Field experiment. Water Resour. Res. 43 (10). https://doi.org/10.1029/2006WR005261.
Holder, C.D., 2003. Fog precipitation in the Sierra de las Minas Biosphere Reserve, Guatemala. Hydrol. Process. 17 (10), 2001–2010. https://doi.org/10.1002/hyp.1224.
Hůnová, I., Brabec, M., Geletič, J., Dumitrescu, A., Malý, M., 2020. Terrain and its effects on fog occurrence. Sci. Total Environ. 10 (768), 144359. https://doi.org/10.1016/j.scitotenv.2020.144359.
Hůnová, I., Brabec, M., Geletič, J., Malý, M., Dumitrescu, A., 2021. Statistical analysis of the effects of forests on fog. Sci. Total Environ. 10 (781), 146675. https://doi.org/10.1016/j.scitotenv.2021.146675.
Iida, S.I., Takeuchi, S., Shinozaki, K., Araki, M., 2022. Calibration of sap flow techniques using the root-ball weighing method in Japanese cedar trees. Trees 36 (6), 1747–1759.
Ingraham, N.L., Matthews, R.A., 1995. The importance of fog-drip water to vegetation: point Reyes Peninsula, California. J. Hydrol. 164 (1–4), 269–285.
Ingwersen, J.B., 1985. Fog drip, water yield, and timber harvesting in the Bull Run Municipal Watershed, Oregon. JAWRA J. Am. Water Resour. Assoc. 21 (3), 469–473.
Johnstone, J.A., Dawson, T.E., 2010. Climatic context and ecological implications of summer fog decline in the coast redwood region. Proc. Natl. Acad. Sci. 107 (10), 4533–4538.
Kassuelke, S.R., Dymond, S.F., Feng, X., Savage, J.A., Wagenbrenner, J.W., 2022. Understory transpiration rates following harvest in a coast redwood forest. Ecohydrology e2404. https://doi.org/10.1002/eco.2404.
Keppeler, E., 2007. Effects of timber harvest on fog drip and streamflow, Caspar Creek Experimental Watersheds, Mendocino County, California. In: Standiford, Richard B., Giusti, Gregory A., Valachovic, Yana, Zielinski, William J., Furniss, Michael J. (Eds.), Proceedings of the Redwood Region Forest Science symposium: What does the Future hold? Gen. Tech. Rep. PSW-GTR-194. Pacific Southwest Research Station, Forest Service, US Department of Agriculture, Albany, CA, pp. 85–94 (Vol. 194).
Keppeler, E., Wagenbrenner, J., Dymond, S., Dralle, D., 2024. Streamflow response to drought in a managed coast redwood forest. J. Am. Water Resour. Assoc. https://doi.org/10.1111/1752-1688.13211.
Keppeler and Ziemer, 1990. Water Resour. Res. 26 (7), 1669–1679.
Klos, P.Z., Goulden, M.L., Riebe, C.S., Tague, C.L., O'Geen, A.T., Flinchum, B.A., Bales, R.C., 2018. Subsurface plant-accessible water in mountain ecosystems with a Mediterranean climate. Wiley Interdiscip. Rev.: Water 5 (3), e1277.
Leopold & Sevens, Inc, 1978. Steven Water Resources Data Book, 3rd Edition. Leopold & Stevens, Inc., Beaverton, OR.
Limm, E.B., Simonin, K.A., Bothman, A.G., Dawson, T.E., 2009. Foliar water uptake: a common water acquisition strategy for plants of the redwood forest. Oecologia 161 (3), 449–459. https://doi.org/10.1007/s00442-009-1400-3.
Liu, Y., Kumar, M., Katul, G.G., Konings, A.G., 2020. Plant hydraulics accentuates the effect of atmospheric moisture stress on transpiration. Nat. Clim. Chang. 10, 691–695. https://doi.org/10.1038/s41558-020-0781-5.
Means, Thos.H., 1927. Fog precipitated by trees. Science 66 (1713), 402–403.
Oberlander, G.T., 1956. Summer fog precipitation on the San Francisco Peninsula. Ecology 37 (4), 851–852. Retrieved from. https://about.jstor.org/terms.
Petreshen, J., 2021. Fog Presence and Ecosystem Responses in a Managed Coast Redwood Forest. University of Minnesota Duluth. Master's Thesis.
Pryet, A., Domínguez, C., Tomai, P.F., Chaumont, C., d'Ozouville, N., Villacís, M., Violette, S., 2012. Quantification of cloud water interception along the windward slope of Santa Cruz Island, Galapagos (Ecuador). Agric. For. Meteorol. 161, 94–106. https://doi.org/10.1016/j.agrformet.2012.03.018.
R Core Team, 2024. R: A language and Environment For Statistical computing. Version 4.4.1. R Foundation for Statistical Computing, Vienna, Austria. ISBN 3-900051-07-0, URL. http://www.R-project.org.
Rastogi, B., Williams, A.P., Fischer, D.T., Iacobellis, S.F., McEachern, K., Carvalho, L., Still, C.J., 2016. Spatial and temporal patterns of cloud cover and fog inundation in coastal California: ecological implications. Earth Interact. 20 (15). https://doi.org/10.1175/EI-D-15-0033.1.
Reid, L.M., Lewis, J., 2009. Rates, timing, and mechanisms of rainfall interception loss in a coastal redwood forest. J. Hydrol. (375), 459–470. https://doi.org/10.1016/j.jhydrol.2009.06.048, 3-4).
Richardson, P.W., Seehafer, J.E., Keppeler, E.T., Sutherland, D.G., Wagenbrenner, J.W., Bladon, K.D., Dymond, S.F., Cole, R.P., 2021. Fifty-eight years and counting of watershed science at the Caspar Creek Experimental Watersheds in northern California. Hydrol. Process. 35 (6), e14207. https://doi.org/10.1002/hyp.14207.
Ritter, A., Regalado, C.M., Aschan, G., 2008. Fog water collection in a subtropical Elfin Laurel forest of the Garajonay National Park (Canary Islands): a combined approach using artificial fog catchers and a physically based impaction model. J. Hydrometeorol. 9 (5), 920–935. https://doi.org/10.1175/2008JHM992.1.
Sawaske, S.R., Freyberg, D.L., 2015. Fog, fog drip, and streamflow in the Santa Cruz Mountains of the California Coast Range. Ecohydrology 8 (4), 695–713.
Sillett, S.C., Antoine, M.E., Carroll, A.L., Graham, M.E., Chin, A.R.O., Van Pelt, R., 2022. Rangewide climatic sensitivities and non-timber values of tall *Sequoia sempervirens* forests. For. Ecol. Manage. 526, 120573. https://doi.org/10.1016/j.foreco.2022.120573.
Simonin, K.A., Santiago, L.S., Dawson, T.E., 2009. Fog interception by Sequoia sempervirens (D. Don) crowns decouples physiology from soil water deficit. Plant Cell Environ. 32 (7), 882–892.
Torregrosa, A., Combs, C., Peters, J., 2016. GOES-derived fog and low cloud indices for coastal north and central California ecological analyses. Earth Space Sci. 3 (2), 46–67. https://doi.org/10.1002/2015EA000119.
Weiss, M., Barat, F., Smith, G.J., Jonckheere, I., Coppin, P., 2004. Review of methods for in situ leaf area index (LAI) determination: part II. Estimation of LAI, errors and sampling. Agric. For. Meteorol. 121 (1–2), 37–53. https://doi.org/10.1016/j.agrformet.2003.08.001.
Werner, Z., Tsz Hin Choi, C., Winter, A., Vorster, A.G., Berger, A., O'Shea, K., Evangelista, P., Woodward, B., 2022. MODIS sensors can monitor spatiotemporal trends in fog and low cloud cover at 1km spatial resolution along the U.S. Pacific Coast. Remote Sens. Appl. Soc. Environ. 28, 100832. https://doi.org/10.1016/j.rsase.2022.100832.
Williams, A.P., Still, C.J., Fischer, D.T., Leavitt, S.W., 2008. The influence of summertime fog and overcast clouds on the growth of a coastal Californian pine: a tree-ring study. Oecologia 156 (3), 601–611. https://doi.org/10.1007/s00442-008-1025.
NCEP/EMCEdited by Xia, Y., et al., 2009. NLDAS primary forcing Data L4 hourly 0.125 x 0.125° V002. In: Mocko, David (Ed.), NASA/GSFC/HSL. Goddard Earth Sciences Data and Information Services Center (GES DISC), Greenbelt, Maryland, USA. https://doi.org/10.5067/6J5LHHOHZHN4. Accessed: July 25, 2024.